Mem. S.A.It. Vol. 90, 366

Memorie della

Towards constraints on massive galactic stars using VLT/SPHERE with high-contrast imaging

A. Rainot[1], M. Reggiani[1], H. Sana[1], C. A. Gomez-Gonzalez[2], O. Absil[3], V. Christiaens[3,4,5], P. Delorme[2], L. Almeida[6,7], S. Caballero-Nieves[8], J. De Ridder[1], K. Kratter[9], S. Lacour[10], J.-B. Le Bouquin[2], L. Pueyo[11], and H. Zinnecker[12]

[1] Inst. of Astrophysics, KU Leuven, Celestijnlaan 200D, 3001 Leuven, Belgium
e-mail: alan.rainot@kuleuven.be
[2] IPAG Université, Grenoble, 38058 Grenoble, France
[3] STAR Institute, Université de Liège, 19 Allée du Six Août, B-4000 Liège, Belgium
[4] Departamento de Astronomía, Universidad de Chile, Casilla 36-D, Santiago, Chile
[5] Millenium Nucleus "Protoplanetary Disks in ALMA Early Science", Chile
[6] Departamento de Física, UERN, Mossoró, RN, Brazil
[7] DFTE, UERN, CP 1641, Natal, RN, 59072-970, Brazil
[8] Dept. of Phys. & Sp. Sci., FIT 150 West University Blvd, Melbourne, FL 32901, USA
[9] Department of Astronomy, University of Arizona, Tucson, AZ 85721, USA
[10] LESIA, (UMR 8109), OBSPM, PSL, CNRS, UPMC, Univ. Paris-Diderot, 5 place Jules Janssen, 92195 Meudon, France
[11] Space Telescope Science Institute, 3700 San Martin Drive, Baltimore, MD, 21218, USA
[12] AIP, An der Sternwarte 16, 14482 Potsdam, Germany

Abstract. While the formation of massive stars remains heavily debated, it is nowadays clear that the formation scenarios need to account for the high-degree of multiplicity of these objects that has been observed by recent studies. Here we introduce the Carina High-contrast Imaging Project for massive Stars (CHIPS) that aims to obtain coronagraphic observations of massive stars in the Carina region using VLT/SPHERE. We illustrate the capabilities of SPHERE for massive stars by focusing on the QZ Car system. We detect 19 sources, most of them for the first time, within a 7x7″field of view. We show that contrast better than 9 mag can be achieved at separation larger than 200 mas. We also investigate avenues to obtain a first characterisation of the detected sources by fitting their source energy distribution with pre-main sequence stellar atmosphere models.

Key words. Stars: massive – Stars: early-type – Stars: individual: QZ Car – binaries: close – binaries: visual – Techniques: high angular resolution Massive Stars: formation – Stars: multiplicity – High-contrast imaging

1. Introduction

The formation of massive stars is one of the most fascinating topics in astronomy today (e.g., Zinnecker & Yorke 2007; Tan et al. 2014). The processes involved are difficult to observe due to several factors: massive stars

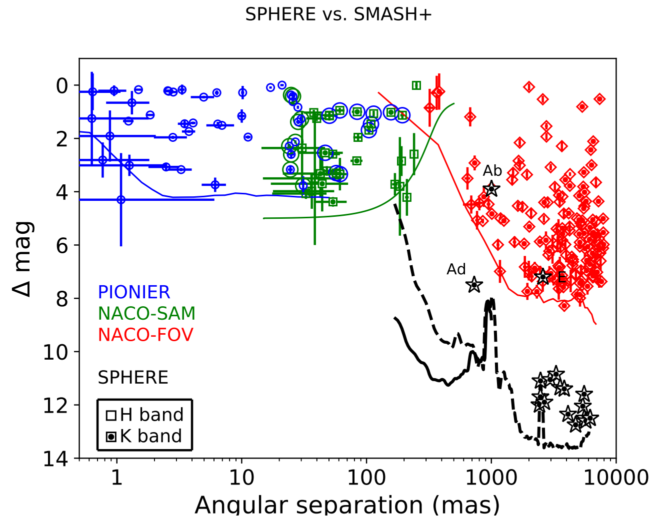

Fig. 1. SMaSH+ (Sana et al. 2014) companion detections in the magnitude contrast vs. angular separation space. Also represented are QZ Car's companions detected with SPHERE (star symbol). The thick lines show the contrast curves limits of the different instruments (see legend).

are rare and found at large distances, their formation timescale is short and the environment in which they are birthed is strongly obscured by gas and dust.

Multiple formation scenarios have been proposed: formation through stellar collisions and merging (Bonnell et al. 1998), competitive accretion (Bonnell et al. 2001; Bonnell & Bate 2006) and monolithic collapse (McKee & Tan 2003; Krumholz 2009). These theories predict that formation disks likely fragment under gravitational instabilities (Kratter et al. 2010). This effect results in the formation of companions but model predictions are few. Therefore by studying the multiplicity of these massive objects, crucial constraints to discriminate between the different formation scenarios of massive stars could be provided.

A few recent surveys have studied the multiplicity properties of massive stars in the Milky Way and nearby galaxies (for a review, see e.g. Sana et al. 2017). These surveys have used different methods to determine the binary fraction of massive stars: some used spectroscopy to study young massive stellar clusters (Sana et al. 2012) and OB associations (Kiminki & Kobulnicky 2012) while others focused on the high-angular resolution observations of massive stars (Mason et al. 2009). Of relevance to this proceeding, two surveys have used high-resolution imaging techniques to uncover properties among massive star populations: the Southern MAssive Stars at High angular resolution survey (SMaSH+ (SMaSH+, Sana et al. 2014) (shown here on Fig. 1) and the HST fine guidance sensor survey (HST-FGS, Aldoretta et al. 2015). On the one hand, SMaSH+ was an ESO VLT Large Program (P89-P91) that combined optical interferometry (VLTI/PIONIER) and aperture masking (NACO/SAM) to search for bright companions ($\Delta H < 4$) in the angular separation regime $0.001'' < \rho < 0.2''$ around a large sample of O-type stars. Using the entire NACO field of view, they also searched for fainter companions ($\Delta H < 8$) up to $8''$. On the other hand, HST-FGS was an all sky survey that used the FGS1r instrument to search for companions of massive stars at separations between $0.01''$and $1''$and brighter than $\Delta m = 5$. They observed 224 O and B type stars and luminous stars in the Large Magellanic Cloud.

The results from the previous surveys show the importance of such studies for the understanding of massive star formation. They concluded that a larger number of faint companions are seen at large separations, corresponding roughly to the outer edge of the accretion disk. These companions may correspond to outward migrating clumps resulting from the fragmented accretion disk or result from tidal capture. Investigating whether low-mass companions exist at closer separations or if there is a characteristic length at which the flux *vs.* separation distribution changes is therefore critical.

The extreme-AO Spectro-Polarimetric High-contrast Exoplanet REsearch instrument (SPHERE, Beuzit et al. 2008) installed at the Unit Telescope 3 of the Very Large Telescope now provides the necessary spatial resolution and dynamics to search for faint companions nearby massive stars. By combining high-contrast imaging observations with state-of-the-art image post-processing algorithms we aim at unveiling the multiplicity properties of massive star in a parameter space uncovered so far.

In this proceeding we present the Carina High-contrast Imaging Project for massive Stars (CHIPS, in Sect. 2) and then focus on QZ Car (Sect. 3), an example star studied within this project.

2. CHIPS

The Carina High-contrast Imaging Project of massive Stars is a high-contrast imaging survey of all O-type stars (90+ stars) within the Carina region down to a magnitude contrast of $\Delta m \approx 14$. This region has the particularity of being a massive factory of massive stars and is the only nearby active star forming region massive enough to provide us with a statistically significant, uniformly selected, large sample. In particular, dwarfs O stars only represented 20% of the SMaSH+ sample because the survey was magnitude-limited ($H < 7.5$). This limit is easily surpassed by SPHERE performances.

Once completed, CHIPS will provide the ultimate data set to establish the multiplicity properties of massive stars in the 450-3000 AU separations, including the properties of the low end of the companion mass function.

Observations were carried out with SPHERE for 43 known O stars in the region (all with estimated initial mass larger than 15 $M_{\odot}$), with an estimated total of 90+ massive stars within a 3°-diameter region around η Car. 70% of this sample is beyond the magnitude limit of SMaSH+. Specifically, our observations were executed in the IRDIFS-EXT mode which combines the Integral Field Spectrograph (IFS, Claudi et al. 2008) and the Infra-Red Dual-beam Imaging and Spectroscopy (IRDIS, Dolhen et al. 2008) sub-systems. IFS images have a size of 290 $\times$ 290 pixels and a pixel size of 7.4 mas with field of view of $1.73'' \times 1.73''$on the sky whereas IRDIS covers a field of $12'' \times 12''$ with a camera size of 1024×1024 pixels and a pixel size of 12.25 mas. The IRDIFS_EXT observation mode enabled us to combine the IFS (YJH bands) and IRDIS (K band) observations to obtain two different fields of view at the same time, giving us two different perspectives on the target. The smaller IFS field-of-view allows us to peer at the close-environment of the star to check for any companions and its spectroscopic ability helps us to characterise any companion present. Meanwhile, IRDIS provides information on the local density of faint objects to obtain statistical evidence of the detected companions with IFS.

Our observations were conducted in pupil tracking mode, where the telescope is fixed on the central star and the sky rotates around it. This allows us to use Angular (ADI) and Spectral (SDI) Differential Imaging techniques, and disentangle the rotation of potential companions from the noise.

During ESO's periods 96, 98 and 102, 43 stars were observed and the data was reduced by the SPHERE Data Center (DC) at the Institut de Planetologie et d'Astrophysique de Grenoble (IPAG). The SPHERE-DC provided us with the science frames consisting of 4D data cubes (wavelengths, rotations and the 2D positions), tables containing the wavelengths and rotational angles, and the 3D PSF cubes (wavelengths and the 2D positions).

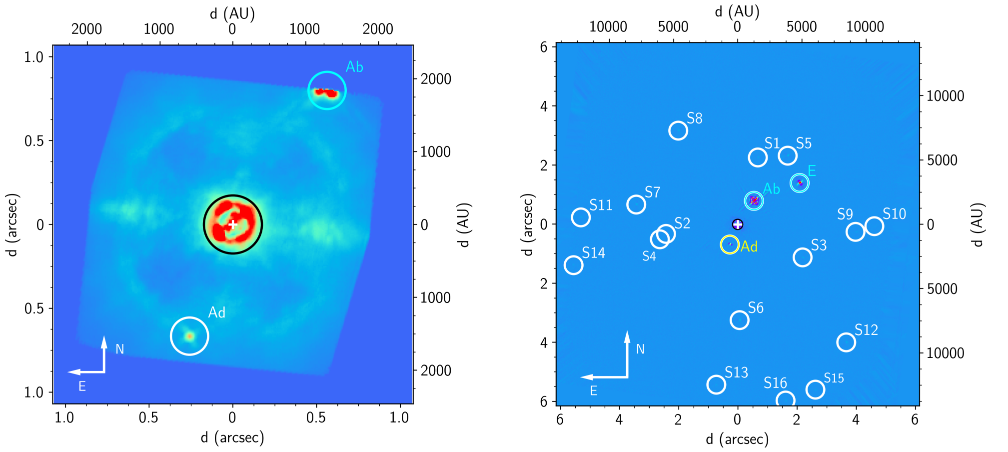

Fig. 2. Post-processed science frames from IFS (left) and IRDIS (right) instruments. Both have angular and spectral differential imaging applied. The two wavelengths K1 and K2 were combined for IRDIS. Dark circles on the images show the 0.173″-diameter size of the coronagraph. The blue circles indicate the previously detected companions Ab and E. White circles indicate the IRDIS sources detected at the 5σ level while yellow circles indicate the new companion QZ Car Ad. The IFS image is 1.73″ × 1.73″; the IRDIS one, 12″ × 12″.

3. QZ Car

QZ Car is a complex multiple system. It is composed by two spectroscopic binaries (Aa & Ac) and three already known companions (Ab, E and B), within 7″ from the centre. The Aa1-Aa2 spectroscopic pair has a spectral type of O9.7I + B2V and an orbital period of 20.7 days. The second Ac1-Ac2 pair is comprised of two stars of O8III and O9V spectral types, respectively, with a period of 6 days. The two spectroscopic binaries are separated by 0.03″(Sana et al. 2014; Sanchez-Bermudez et al. 2017) with combined magnitudes of 5.393 and 5.353 in H and Ks-band, respectively. In addition to this system, the SMaSH+ survey found three companions orbiting around it: Ab, E and B at separations of of 1″, 2.58″and 7.07″from QZ Car, respectively.

Our observations were conducted with SPHERE in January 2016 and from the SPHERE-DC we obtained the reduced science frames with 48 rotations, 39 wavelength channels and positions and the PSF frames with 3 images, 48 rotations and 2D positions. Tables with wavelengths and rotations were also provided.

3.1. Data reduction

After obtaining the data from the SPHERE-DC, we made use of the spectral and angular information of our observations in order to increase the contrasts and suppress artefacts from the data. For this purpose, high-contrast imaging techniques such as ADI and SDI with Principal Component Analysis (PCA, Amara & Quanz 2012; Soummer et al. 2012) were employed. These techniques enabled us to reach a high-contrast and better signal-to-noise level in our observations. We made use of the Vortex image Processing package (VIP, Gomez Gonzalez et al. 2017) and pyKLIP (Wang et al. 2015) for this endeavour. pyKLIP finds the accurate locations of companions and VIP works on the detection and characterisation of those companions.

In Fig. 2 we have applied ADI-SDI with a principal component of 1 on SPHERE observations of QZ Car with IFS and IRDIS. On the IFS image, the central star is at the centre of the image and is blocked by the coronagraph and right below it, there is a bright source. This object will extensively be presented in this proceeding. By eye from these images, many bright features already appear in the image and we explain our methods of identifying companions and characterising them in the next section.

3.2. Detection

To identify real companions, we first estimated the signal-to-noise ratio (S/N) of each pixel in the images and applied a threshold to detect any source at a given S/N limit. This is done with VIP which outputs a S/N map. Setting the limit to 5σ, we detected again the previous Ab and E companions, the new Ad source but as well as 16 other companion candidates in the IRDIS image only (Fig. 2). Therefore in total there are 19 sources detected in a radius of 6″around QZ Car. Some of these detected stars may be spurious associations and we can compute a probability for this association but results and the discussion about this topic will be presented in Rainot et al. (*in prep.*).

3.3. Source characterisation

Following the detection of candidate companions, we then proceeded to characterising extensively Ad and attempted to constrain properties for the other sources. Making use of VIP, the fluxes of companions were extracted in each wavelength channel using both a Simplex Nelder-Mead optimisation and a Markov-Chain-Monte-Carlo (MCMC). The latter proved to be computer-intensive and provided very similar results compared to the faster Simplex method. We therefore obtained an uncalibrated spectrum with 39 channels for Ad in the IFS dataset and two flux values for IRDIS sources.

We also applied these methods to the PSF images of QZ Car for the IFS and IRDIS which enabled us to obtain reference fluxes at each wavelength channel. To obtain the contrast fluxes, we divided the flux values of IFS and IRDIS obtained with VIP by the spectrum of the PSF.

The contrast fluxes only give us information on the relative difference in brightness between the central star and the companions but in order to characterise these companions, a calibrated spectrum of the central star is required. Missing such a YJH spectrum of the central star, we modelled the components of QZ Car separately using a non-Local Thermodynamic Equilibrium (non-LTE) atmosphere code named FASTWIND (Puls et al. 2005; Rivero-González et al. 2011), and added the contribution of each of these components to obtain a model of QZ Car's spectrum.

With such a model calibrated spectrum of the central QZ Car system, we then multiplied this spectrum by the contrast spectrum obtained previously for Ad and the resulting flux-calibrated spectrum is the one shown on Fig. 3.

3.4. Results

3.4.1. Physical properties of of QZ Car Ad

With a flux-calibrated spectrum of the companion Ad, we are able to fit model spectra from different Spectral Energy Distribution (SED) libraries available in order to constrain the stellar parameters of Ad. For this purpose we used the ATLAS9 LTE atmosphere models (Castelli & Kurucz 2004) along with the pre-main sequence (PMS) evolutionary tracks of Siess et al. (2000) and compared them to the SED of Ad. We computed the χ^2 at each step to get the best-fit results. We omitted the three data points corresponding to the strong telluric region which sits between the $J-$ and $H-$ bands between 1.35 and 1.40 μm during the rebinning process for the ATLAS9 models into IFS wavelength channels when we calculated the χ^2. The resulting χ^2 region is shown in Fig. 4.

There are several possible good-fits but the mass remains limited to the range between 2 and 2.2 $M_\odot$. The best fit is found for a star with $T_{\rm eff}$ = 9600 K, $\log g$ = 4.28 and R = 1.77 $R_\odot$ and a mass of 2.2 $M_\odot$. According to Siess et al. (2000) evolutionary tracks, this star corresponds to ZAMS or an early-main sequence star. Its estimated age is 7.7 Myr and is in qualitative agreement with estimates of QZ Car's age (Walker et al. 2017). The best-fit model is shown in Fig. 3 and shows that the model SED found matches well the observed spectrum of

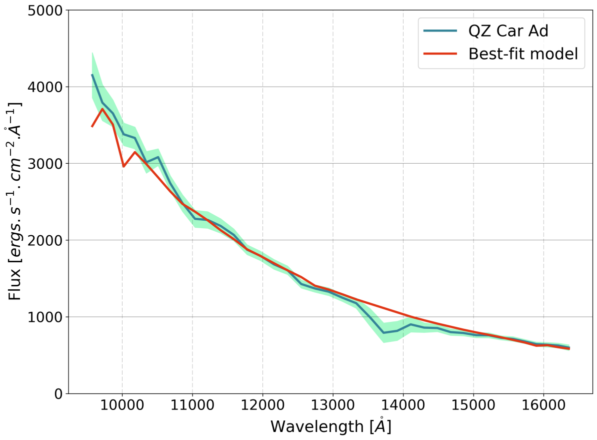

Fig. 3. Flux-calibrated IFS spectrum of QZ Car Ad. The red line corresponds to an ATLAS9 model with $T_{\rm eff}$ = 9500 K, $\log g$ = 4.25 and R = 1.8 $R_\odot$. Shaded green line shows the 1σ uncertainties. The green spectrum was computed at a distance of 100 $R_\odot$ from the star.

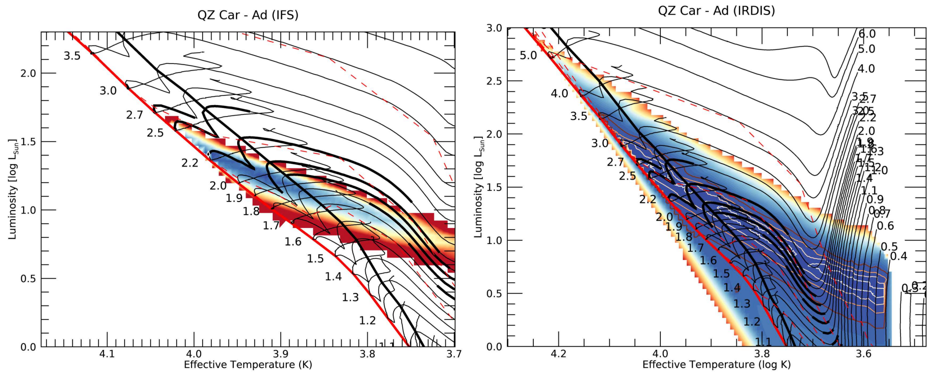

Fig. 4. *Left:* χ^2-surface resulting from ATLAS model fit to Ad's IFS SED projected on to the HRD plane. The thick black and red lines are ZAMS and early-MS according to Siess et al. (2000) definitions. Thin black lines are the evolutionary PMS tracks for stars with masses increasing from bottom to top from 1.1 to 3.5 $M_\odot$. The 4 to 8 Myr parts of the respective evolutionary tracks are displayed with a thicker line. Finally, dashed line give, from top to bottom, the 1, 5 and 10 Myr isochrones. *Right:* Same for the IRDIS observations of QZ Car Ad. White contours give the 68 and 95% confidence regions, providing constraints in qualitative agreement with the IFS results of the left-hand panel. From Rainot et al. (submitted).

Ad. The models are also represented on Fig. 4. According to Siess et al. (2000) tracks, Ad corresponds to a A0 or A1 type star.

3.5. Multiplicity results

In total we have 40 stars already observed in periods 96, 98 and 102 with 53 remaining to be observed (submitted). From these observations, we obtained preliminary detections of 17 candidates within the IFS field-of-view. Most of these companions have a magnitude contrast of 6 and are in the range $0.15'' < \rho < 0.8''$. Assuming that the detection rate remains the same for the remaining 53 stars to observe, we expect a total of $\sim$ 40 companions within the CHIPS project, which is enough to populate the parameter space and robustly check for (anti-) correlations between separation and magnitudes predicted by theory.

4. Conclusions

We have presented the CHIPS project which aims to obtain the multiplicity properties of all O and WR stars within the Carina region, totalling 93 massive targets, using the latest high-contrast imaging techniques with the SPHERE instrument. SPHERE was set to the IRDIFS_EXT mode which makes use of both IRDIS and IFS sub-instruments and so far we have obtained the observations of 40 stars from this survey. The case of the complex system QZ Car was described: 19 sources (including two previously known Ab and E) were detected within the IRDIS field-of-view and a new close companion, named Ad, was discovered at 729.1 mas. This companion was extensively analysed and using the high-contrast imaging software VIP and pyKLIP, we were able to extract a spectrum from the 39 wavelength channels in IFS and two flux values for IRDIS. By finding the contrast spectrum and multiplying it by a flux-calibrated model of the central system's spectrum, we were able to get a flux-calibrated spectrum of companion Ad.

We compared the spectrum with LTE ATLAS9 library of SED models along with Siess et al. (2000) evolutionary tracks and computed a χ^2 for every wavelength channel. This gave us the best fit physical properties for Ad: this companion is between an A0 to an A1 star of mass $2.2\,M_\odot$, $T_{\rm eff} = 9600$ K, $\log g = 4.28$ and $R = 1.77\,R_\odot$.

As well as detecting the companion candidates with IRDIS, IFS helped us in characterising these companions and gives us some physical properties for these companions.

Future prospects would include the analysis of the entire survey sample, which would give us a direct evidence of multiplicity in the products of massive star formation. Higher resolution spectra for those companions may be possible thanks to the IRDIS Long Slit Spectroscopy mode which increases the resolution from 39 channels to 350, providing crucial detail into the emission and absorption lines.

As shown in this proceeding, SPHERE opens a new window into the discovery space of low-mass and faint companions around massive stars. Its high-contrast capabilities enables the thorough investigation of previously undetected companions providing us with essential information required to better understand the outcome of massive star formation.

Acknowledgements. We acknowledge the support from the FWO-Odysseus program under project G0F8H6N. This project has further received funding from the European Research Council under European Union's Horizon 2020 research programme (grant agreement No 772225-COG MULTIPLES). This work is based on observations collected at the European Southern Observatory under programs ID 096.C-0510(A). We thank the SPHERE Data Centre, jointly operated by OSUG/IPAG (Grenoble), PYTHEAS/LAM/CeSAM (Marseille), OCA/Lagrange (Nice) and Observatoire de Paris/LESIA (Paris) and supported by a grant from Labex OSUG@2020 (Investissements davenir ANR10 LABX56). We especially thank P. Delorme and E. Lagadec (SPHERE Data Centre) for their help during the data reduction process. JDR acknowledges the BELgian federal Science Policy Office (BELSPO) through PRODEX grants *Gaia* and PLATO.

References

Aldoretta, E.J., et al. 2015, ApJ, 149, 26

Amara, A., & Quanz, S. P. 2012, MNRAS, 427, 948

Beuzit, J.-L., et al. 2008, Proc. SPIE, 7014, 701418

Bonnell, I.A., Bate, M.R., Zinnecker, H. 1998, MNRAS, 298, 93

Bonnell, I.A., et al. 2001, MNRAS, 323, 785

Bonnell, I.A., & Bate, M.R. 2006, MNRAS, 370, 488

Castelli, F., & Kurucz, R. L. 2003, in Modeling of stellar atmosphers, eds. N. Piskunov et al. (ASP, San Francisco), IAU Symp., 210 A20 [arXiv:astro-ph/0405087]

Claudi, R.U., et al. 2008, Proc. SPIE, 7014, 70143E

Dohlen, K., et al. 2008, Proc. SPIE, 7014, 70143L

Gomez Gonzalez, C. A., Wertz, O., Absil, O., et al. 2017, ApJ, 154, 7
Kiminki, D.C., Kobulnicky, H.A. 2012, ApJ, 751, 1
Kratter, K.M., et al. 2010, ApJ, 708, 1585
Krumholz, M.R. 2009, Science, 323, 754
Mason, B.D., et al. 2009, ApJ, 137, 3358
McKee, C.F., Tan, J.C. 2003, ApJ, 585, 850
Puls, J., et al. 2005, A&A, 435, 669
Rivero-González, J. G., Puls, J., Najarro, F. 2011, A&A, 536, A58
Sana, H., De Mink, S.E., de Koter, A., et al. 2012, Science, 337, 444
Sana, H., Le Bouquin, J.-B, Lacour, S., et al. 2014, ApJ, 215, 1
Sana, H., et al. 2017, A&A, 599, L9
Sanchez-Bermudez, J., Alberdi, A., Barbá, R., et al. 2017, ApJ, 845, 57
Siess, L., Dufour, E., Forestini, M. 2000, A&A, 358, 593
Soummer, R., Pueyo, L., & Larkin, J. 2012, ApJ, 755, L28
Tan, J. C., Beltrán, M. T., Caselli, P., et al. 2014, in Protostars and Planets VI, eds. Beuther et al. (Univ. Arizona Press, Tucson), 149
Walker, W. S. G., et al. 2017, MNRAS, 470, 2
Wang, J. J., Ruffio, J.-B., De Rosa, R. J., et al. 2015, Astrophysics Source Code Library, ascl:1506.001
Zinnecker, H., & Yorke, H. W. 2007, ARA&A, 45, 481